Journal of Materials Chemistry A

One-pot synthesis of nitrogen and phosphorus-dual-doped carbon nanotube array as highly effective electrocatalyst for oxygen reduction reaction

Journal:	*Journal of Materials Chemistry A*
Manuscript ID:	TA-ART-05-2014-002427.R1
Article Type:	Paper
Date Submitted by the Author:	18-Jul-2014
Complete List of Authors:	Zhu, Jinliang; SUN YAT-SEN UNIVERSITY, Jiang, San Ping; Curtin University of Technology, Department of Chemical Engineering wang, ruihong Shi, Kaiying; Heilongjiang University, Shen, Pei; Sun Yat-sen University,

SCHOLARONE™
Manuscripts

Journal of Materials Chemistry A

Dynamic Article Links ►

Cite this: DOI: 10.1039/c0xx00000x

www.rsc.org/xxxxxx

Paper

One-pot synthesis of nitrogen and phosphorus-dual-doped carbon nanotube array as highly effective electrocatalyst for oxygen reduction reaction

Jinliang Zhu[a], San Ping Jiang[*, b], Ruihong Wang[c], Keying Shi[c] and Pei Kang Shen[*, a]

Received (in XXX, XXX) Xth XXXXXXXXX 20XX, Accepted Xth XXXXXXXXX 20XX
DOI: 10.1039/b000000x

A nitrogen and phosphorus-dual-doped carbon nanotube (N, P-CNT) array has been successfully synthesized by a novel one-pot method, using aminophosphonic acid resin as the N, P and C sources. The N, P-CNTs are open with large inner channels, allowing oxygen molecules to access a large number of catalytically active sites on inner walls. The N, P-CNTs are not only comparable to Pt/C in electrocatalytic activity for oxygen reduction reaction (ORR) in 0.1M KOH, but are also highly stable and tolerant to methanol and CO poisoning. An onset potential of 0.95 V closing that of Pt/C and a well-defined limiting current plateau for the ORR are observed. Moreover, there is almost no visible current density decrease on N, P-CNTs after 5,000 cycles.

GA image

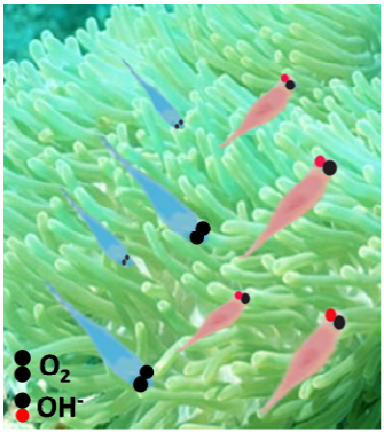

The N, P-dual-doped CNTs with a robust nano-structure has been synthesized by one-pot method and the material shows enhanced activities and durability for oxygen reduction reaction.

1 Introduction

Considerable efforts have been devoted to synthesize hollow nanostructured carbon materials such as fullerenes[1], carbon nanotubes[2, 3], nanoshell[4], carbon nanocages[5] and nanocones[6] for their specific architectures and unique physical and chemical properties. Carbon nanotubes (CNTs), one of the most important hollow nanostructured carbon materials, exhibit potential applications in hydrogen storage[7], lithium-ion batteries (LIBs)[8], supercapacitors[9], nanocontainer and nanoreactor[10, 11] and fuel cells[12, 13]. It has been reported that doped carbon materials by heteroatoms such as nitrogen, boron, phosphorus, sulfur and fluorine have high electrocatalytic activity, high durability and high tolerance towards poisoning of the oxygen reduction reaction.[14-18] Dai et al.[3] showed that nitrogen-doped CNT (N-CNT) array has high electrocatalytic activity for the oxygen reduction reaction in alkaline solutions. Recently, Dai et al.[15] exhibited that CNTs array co-doped with N and P has significantly enhanced electrocatalytic activity towards ORR compared with CNTs doped by N or P only due to the synergetic effect. Doping with heteroatoms can modulate the structure, electronic and physicochemical properties of carbon materials like CNTs. For example, the incorporation of nitrogen atoms into CNTs can activate the π electrons of carbon by the conjugation with the lone-pair electrons of N dopants and significantly increase active sites for the ORR.[19, 20] ORR at the cathode of fuel cells plays a key role in the performance of fuel cells.

Doping CNTs by N or P can be achieved via 'in situ' doping and 'post-synthesis treatment' methods. [21, 22] However, for in situ doping methods, such as arc-discharge, CVD and laser ablation, special instrumentation or rigorous condition control is often required.[21, 23, 24] The method of post-synthesis treatment requires toxic nitrogen precursors (e.g., NH_3).[21] Moreover, the ORR activities of majority of reported N-CNTs are still not satisfactory as compared to Pt-based catalysts. Architecture or nano-structure of CNTs plays an important role in the electrocatalytic activity of N-CNTs. For example, N-CNTs[25, 26] and N, P-dual-doped CNTs[15, 27] having bamboo-like structure and nodes could reduce the catalytic active sites in inner walls by blocking their access to oxygen molecules. On the other hand, less catalytically active sites may lead to a two-electron oxygen reduction pathway, forming intermediate H_2O_2 species, which reduces the electrocatalytic efficiency as well as the stability of catalysts.[28] Therefore, it is of scientific and technological importance to develop novel and facile strategies to synthesize N and P-dual-doped CNTs with robust nano-structure for enhanced activities and durability for ORR.

Herein, for the first time, we report a facile and one-pot synthesis of nitrogen and phosphorus-dual-doped carbon nanotube (N, P-CNT) array with simultaneous nitrogen and phosphorus doping by pyrolysis of nitrogen and phosphorus-containing resin in the presence of nickel foam. Due to the available catalytic active sites in inner walls and the synergetic effect arising from co-doping CNTs with both P and N, the N, P-CNT array shows superior ORR activity with respect to bamboo-like N-CNTs. The N, P-CNTs catalyst provides sufficient catalytically active sites, therefore, showing an excellent electrocatalytic performance for ORR in terms of electrocatalytic activity and stability in an alkaline medium.

2 Experimental section

2.1 Synthesis of N, P-CNT array

The as-received aminophosphonic acid resin (APAR, Sunresin New Materials Co. Ltd., China) was cleaned with deionized water and then dried before using. The treated resin (1.5 g) was placed in a clean quartz boat and the boat was capped with a nickel foam. The boat was then heated to 850 °C at a heating rate of 3 °C min^{-1} and held for 30 min in a tube furnace in N_2 atmosphere. After cooling down to room temperature, the nickel foam was treated with diluted hydrochloric acid to remove nickel substrates and then the N, P-CNTs were collected. The N-doped CNTs (N-CNTs) were also synthesized for comparison. Commercial carbon nanotubes (CNTs) with purity of > 95 % (Shenzhen Nanotech Co., Ltd., China) and Pt/C (46.7 wt% Pt, TKK, Japan) catalysts were used as received.

2.2 Physical characterization

The Raman spectroscopic measurements were carried out on a Raman spectrometer (Renishaw Corp., UK) using a He–Ne laser with a wavelength of 514.5 nm. The X-ray photoelectron spectroscopy (XPS) measurements were performed in an ESCALAB 250 spectrometer under vacuum (about 2×10^{-9} mbar). Monochromatic Al Kα (150 W, 1486.6 eV) was used as the excitation source. All the binding energies were calibrated with respect to C1s peak at 284.8 eV. The morphology characterizations were performed on a scan electron microscopy (SEM) (Quanta 400 FEG, FEI Company). The transmission electron microscopy (TEM) and element mapping investigations were carried out on a JEOL JEM-2010 (JEOL Ltd.) operating at 200 kV and FEI Tecnai G2 F30.

2.3 Electrochemical characterization

The performance of the N, P-CNTs for ORR was measured on a rotating ring-disk electrode (RRDE) with a bipotentiostat (Pine Instrument Co., USA) in a three-electrode cell by using a reversible hydrogen electrode (RHE) as the reference electrode, and a graphite electrode as the counter electrode. The working electrode was a rotating ring/disk electrode with a glassy carbon disk (5.61 mm in diameter). 5.0 mg of N, P-CNTs (N-CNTs or CNTs) was added into 1.9 mL ethanol and 0.1 mL Nafion solution (5 wt%, DuPont, USA) and ultrasonicated for 30 min to form a well-dispersed ink. The ink (100 μL) was transferred onto the surface of the glass carbon electrode and then dried under infrared lamp for 5 min to obtain a catalyst thin film. The total Pt loadings were controlled at 0.0101 mg cm^{-2}. The ORR tests were performed with a scan rate of 5 mV s^{-1} in an O_2-saturated 0.1 mol L^{-1} KOH solution at 25 °C. The rotating speed was controlled at 1600 rpm. In the RRDE tests, the ring potential was set to 1.2 V *vs.* RHE.

3 Results and Discussion

This journal is © The Royal Society of Chemistry [year]

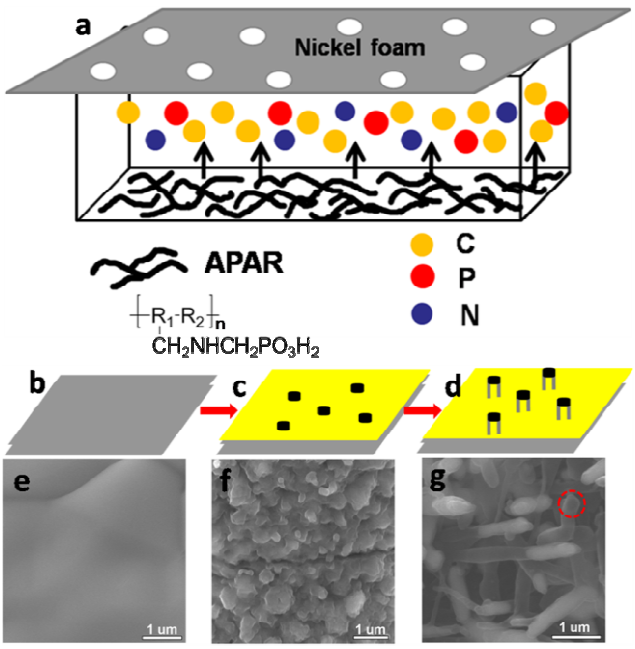

Fig. 1 Schematic illustration of the growth process of N, P-CNT array and SEM images of growing N,P-CNTs at different stages (a, arrangement of the APAR and Ni foam as substrate, b, initial Ni foam substrate, c, Ni foam at 850 °C for 1 min and d, Ni foam at 850 °C for 15 min).

Fig. 1 and Fig. S1 (Supporting Information) show the principle of the growth process of the N, P-CNT array, using aminophosphonic acid resin (APAR) precursor. The APAR precursor was decomposed in N_2 at 325 °C, providing nitrogen, phosphorus and hydrocarbon sources for the growth of N, P-CNT array (Fig. 1a). As temperature arises, the released phosphorus species reacted with clean nickel foam (Fig. 1b), forming rod-like Ni_2P particles[29, 30] on the surface of nickel foam (Fig. 1c). The rod-like Ni_2P particles served as seeds to catalyze the growth of carbon nanotubes (Fig. 1d). As the Ni_2P catalyst particles are most likely located at the tip of carbon tubes, the growth process may follow the 'adsorption-diffusion-precipitation model' in CVD method using metal particles as catalysts.[31, 32] The hydrocarbons released by the resin would adsorbed on the surface of Ni_2P particles and the carbon diffusion and consequent precipitation would lead to the growth of carbon nanotubes with simultaneously doping of N and P. Such simultaneous growth mechanism of N, P-CNTs is further confirmed by the element mapping investigations (Fig. 2). Ni and P are mainly accumulated at the tip of the tube (Fig. 2), indicating that nickel was pulled away from the Ni foam substrate by the formation of Ni_2P seeds, which is confirmed by XRD in Fig. S2. The uniform distribution of N and in less degree of P along the carbon tubes confirms the simultaneously doping of N and P during the growth of carbon tubes.

The production of high density rod-like Ni_2P particles with uniform size is critical to grow such N, P-CNT array. Very different from bamboo-like N-CNTs, where asymmetric metal catalyst particles would lead to the accumulation of carbon at graphite-catalyst edges and consequently the formation of nodes[33-35], the cylindrical Ni_2P rod catalysts avoid the formation of nodes. This is indicated by the growth of very uniform and hollow N, P-CNTs (Fig. 1g). The one-pot synthesis strategy designed for the growth of N, P-CNT arrays has significant advantages over conventional *in-situ* doping or post-synthesis methods. First, the use of APAR provides a low cost and environmentally friendly way for the carbon, nitrogen and phosphorus resource, and requires no special instruments or rigorous conditions. Second, the rod-like Ni_2P particles as catalyst seeds are formed *in situ* and high density and uniform formation of such rod-like seeds prevent formation of bamboo-like structure and nodes. Third, P and N atoms are simultaneously incorporated into the CNTs during the tube growth, eliminating the post-synthesis or extra doping processes.

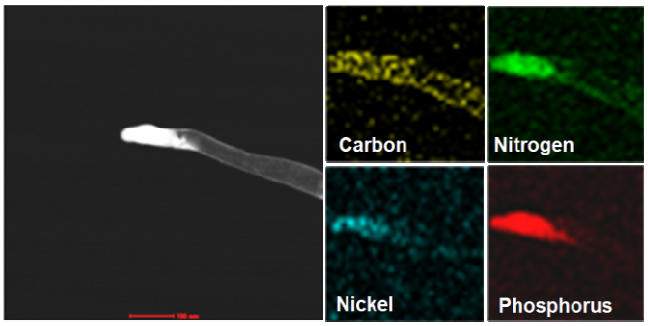

Fig. 2 TEM image (the bar is 100 nm) and corresponding element mappings of a growing N, P-CNT.

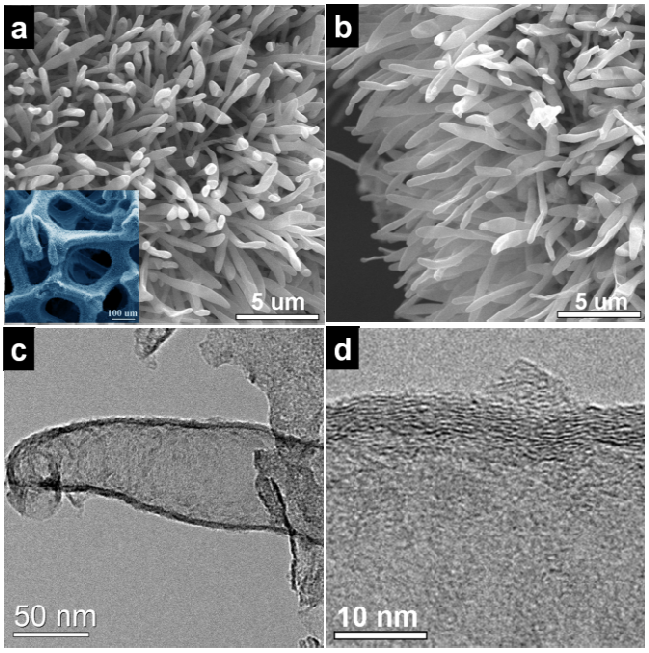

Fig. 3 SEM and TEM images of the N, P-CNT array: (a) Top view and (b) side view. (c) TEM and (d) HRTEM image of an individual N, P-CNT. The inset in (a) is overall view of the N, P-CNTs.

As shown in the inset of Fig. 3a, the overall view of the nickel foam substrates covered with compact and uniform N, P-CNTs,

and formed coral-like array. The magnified SEM images show that the N, P-CNT has noodle-like shape and a length of 20-30 micrometers (Fig. S3). The N, P-CNTs are vertically aligned, and some adjacent N, P-CNTs may be in contact along the length of the array. The N, P-CNTs show bigger tube with diameter of about 100-200 nm (Fig. 3a and 3c), as compared to the conventional multi walled carbon nanotubes (MWCNTs).[36, 37] The N, P-CNT formed by the one-pot synthesis method is also characterized by open end structure (Fig. 3c). It can be observed that defects and distortions in the carbon lattice of the wall, as shown in Fig. 3d. The wall thickness of the tube is about 4.5 nm and ratio of internal diameter to wall thickness can be as high as 20. In contrast, the synthesized N-CNTs show typical bamboo-like structure as shown in Fig. 4. From the SEM image of the N-CNTs, the N-CNTs grow randomly. Thick wall and nodes can be clearly observed in the TEM image of a single N-CNT.

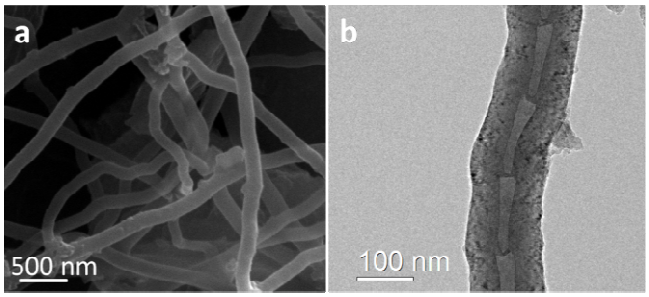

Fig. 4 SEM and TEM images of the N-CNTs.

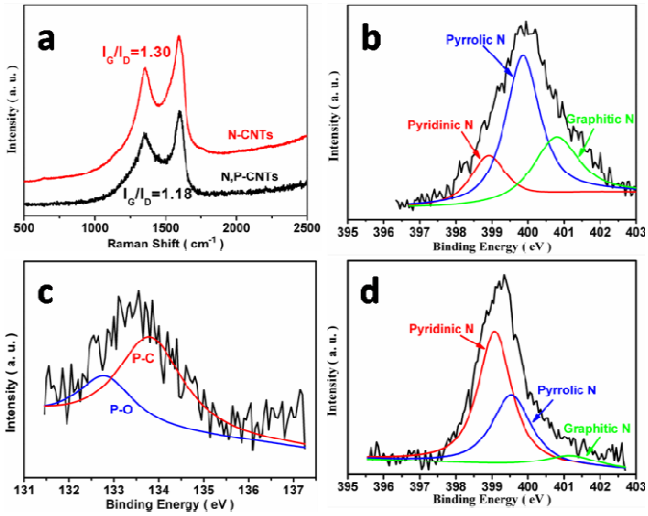

Fig. 5 (a) Raman spectra of the N, P-CNTs and N-CNTs, (b) XPS-N1s spectrum of the N-CNTs, (c) XPS-P2p and (d) XPS-N1s spectrum of the N, P-CNTs.

Table 1 XPS analysis of the samples

Sample	Nitrogen (at. %)	Phosphorus (at. %)
N-CNTs	4.90	0
N, P-CNTs	4.17	4.28

Fig. 5a shows the Raman spectra of N, P-CNTs and N-CNTs in the range of 500-2500 cm^{-1}. The band observed at about 1358 cm^{-1} is assigned to the D-band, which originates from defects in the hexagonal sp^2 carbon network. The appearing band at 1580 cm^{-1} is assigned to the G-band reflecting the structural intensity of the sp^2-hybridized carbon atom.[38, 39] The intensity ratio of the G-band to D-band (I_G/I_D) is approximately 1.18, which is little lower than that of N-CNTs. It may attribute to the doping with P induces defect sites and destruction in the carbon lattice, which leads to increase in degree of distortion.

Fig. 5b and 5d show N1s spectra of the N-CNTs and N, P-CNTs, respectively, which can be further deconvoluted into three peaks[40, 41]: the peak at 398.7 eV can be attributed to pyridinic nitrogen, which is bonded to two carbon atoms and exists on the edge of graphite planes. The peaks located at 399.6 and 401.2 eV can be assigned to pyrrolic nitrogen and graphitic nitrogen, respectively. The pyridinic-N with a lone electron pair in the plane of carbon matrix induces the side-on adsorption during chemisorption of oxygen on the surface of the catalyst, which effectively weakens the O–O bond and facilitates the reduction of O_2.[42, 43] The graphitic nitrogen atoms also could be ORR active and catalyze the ORR through a direct four-electron pathway. The N1s peak clearly shifts to a lower binding energy from N-CNTs to N, P-CNTs, which is attributed to the electron transfer to N and increases the electron density on N for a high electron-donating ability of P. The P2p spectrum of N, P-CNTs (Fig. 5c) can be resolved into two different peaks at the binding energies of 132.8 and 134.0 eV, corresponding to P–O and P–C respectively.[44, 45] The N and P doping levels of N-CNTs to N, P-CNTs are shown in Table 1. Phosphorus, one of the N-group elements, shows similar chemical properties as N and leads to synergistic effects between the dopants.[46, 47] P with larger atomic radius and higher electron-donating ability trends to induce more defects and structural corruption, which increases active sites for ORR and improves electrocatalytic activity.[45, 48]

The electrocatalytic activities of as-synthesized N, P-CNTs for oxygen reduction reaction are shown in Fig. 6 and Fig. S4. For the purpose of comparison, the performances of N-CNTs, commercial CNTs and Pt/C (46.7 wt% Pt, TKK, Japan) catalysts for ORR are also given. The ring current increases dramatically on CNTs at the oxygen reduction potential region (Fig. 6a), which indicates more HO_2^- generated by a two-electron reduction of oxygen. However, the ring current is negligible for the ORR on N, P-CNTs. The onset potential on N, P-CNTs is 0.95 V *vs.* RHE, very closes the onset potential of the Pt/C catalyst. Most importantly, the half wave potential of the reaction on the N, P-CNTs is 0.79 V *vs.* RHE, almost the same as that on the Pt/C catalyst (0.795 V). The remarkable electrocatalytic activity of N, P-CNTs for ORR is not only attributed to N, P-dual doping which can change the net charge of adjacent carbon atoms to facilitate the ORR but also its unique architecture. The open-end N, P-CNT has large amount of the hollow channels and inner walls, which increase the active sites compared with bamboo-shaped N-doped CNT.

This journal is © The Royal Society of Chemistry [year]

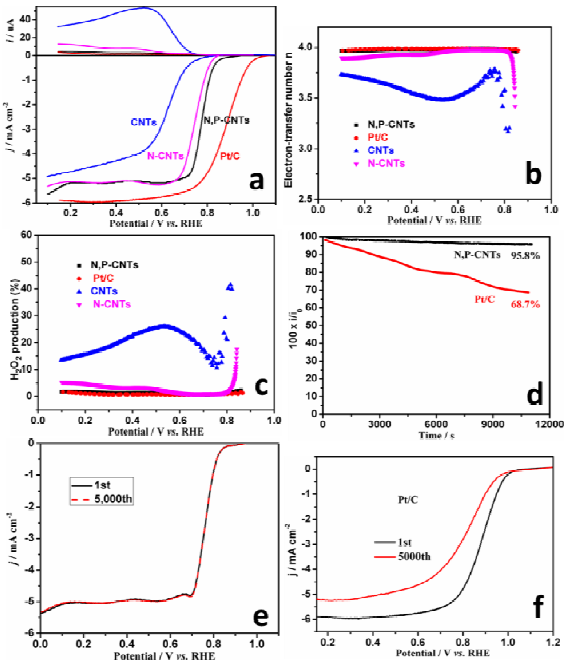

Fig. 6 (a) The linear sweep curves (down) of the catalysts on RDE for ORR and corresponding ring currents (up) at 1600 rpm in O_2-saturated 0.1 mol L^{-1} KOH at 25 °C with a sweep rate of 5 mV s^{-1}, (b) electron-transfer number *n* of the catalysts at different potentials, (c) calculated H_2O_2 production yields of the catalysts, (d) constant potential polarization curves of the N, P-CNTs and Pt/C at constant potential of 0.7 V *vs.* RHE and (e, f) ORR performance of the N, P-CNTs and Pt/C before and after 5,000 cycles in 0.1 mol L^{-1} KOH.

As shown in Fig. 6b and 6c, the electron-transfer number *n* and H_2O_2 production yields of the CNTs, N-CNTs, N, P-CNTs and Pt/C during the ORR can be calculated according to the following equations[49]:

$$n = \frac{4I_D}{I_D + (I_R / N)}$$

$$\%H_2O_2 = 100\frac{(4-n)}{2}$$

where *n* is the apparent electron-transfer number and $\%H_2O_2$ is the percentage of the electron used to generate the H_2O_2 during the ORR, I_D the absolute value of the Faradaic current at the disk, I_R the absolute value of the ring current and *N* the collection efficiency. Obviously, the *n* value was calculated to be from 3.95 to 3.97 and the H_2O_2 produced is below 3 % at potentials from 0.1 V to 0.85 V *vs.* RHE, indicating a high selectivity of O_2 reduction to H_2O through a four-electron route on the N, P-CNTs, similar to that on Pt/C catalysts. The CNTs and N-CNTs catalysts showed more H_2O_2 generated especially at high potentials. The stability of the N, P-CNTs and Pt/C catalysts were evaluated by chronoamperometric experiments at 0.7 V *vs.* RHE (Fig. 6d). Based on the normalized current plots, the loss in the current density for the ORR on N, P-CNTs is only 4.2 % after 3 h polarization, while, in the case of the Pt/C lost 31.3%. After continuous potential cycling, there is no visible current density decrease on N, P-CNTs after 5,000 cycles (Fig. 6e), indicating the high durability of N, P-CNTs as ORR catalysts. However, significant decrease in current density and obvious shift in half wave potential (Fig. 6f) are observed on the Pt/C catalyst. It further indicates that N, P-CNTs has superior ORR stability compared with Pt/C catalyst.

We further evaluate the stability of the N, P-CNTs catalyst by an accelerated test in same media. After 2500 pulse potential cycles (30-60 s alternatively at 0.65 and 1.05 V/RHE) in 0.1 mol/L KOH, very little decrease in current density and almost no shift in half wave potential were observed on the N, P-CNT catalyst, indicating that the N, P-CNTs is very stable for ORR.

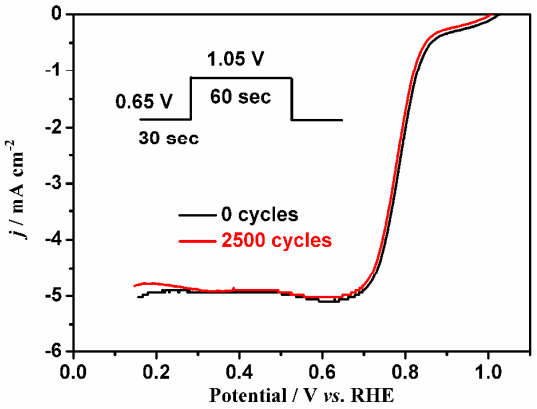

Fig. 7 The stability test of the N, P-CNTs catalyst.

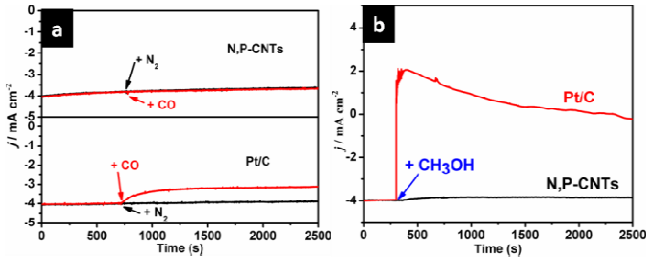

Fig. 8 (a) Constant potential polarization curves of the N, P-CNTs and Pt/C at 0.7 V *vs.* RHE in O_2-saturated 0.1 mol L^{-1} KOH solution with addition of N_2 (black line) and CO (red line) and (b) with addition of 1.0 mol methanol.

The N, P-CNTs catalyst also shows remarkable resistance and tolerance towards methanol and poisoning species of CO for ORR compared to Pt/C (Fig. 8). The Pt/C shows a significant current decay with the addition of CO into the electrolyte. However, in the case of N, P-CNTs, the effect of addition of CO on the polarization current is negligible (Fig. 8a). Similar results are observed for the introduction of methanol into the solution for ORR. Upon addition of 1.0 mol methanol to the O_2-saturated

solution, a sharp positive current increase occurs on Pt/C catalysts, indicating a rapid decay in activity (Fig. 8b). However, the change in the current density is negligible for the ORR on the N, P-CNTs after the introduction of methanol.

4 Conclusions

In summary, we have successfully demonstrated a novel one-pot approach to synthesize N, P-dual-doped CNT array as highly active electrocatalyst for ORR. The N, P-CNTs with open ends and large hollow channels provide a large number of catalytic active sites in inner walls allowing the access of oxygen molecules, such a significant advantageous architecture is superior as compared with conventional bamboo-shape N-CNT and bamboo-shaped N, P-dual-doped CNTs. The comparable activity and much better methanol and CO tolerance for ORR as compared to Pt/C catalyst can be attributed to both the synergistic effect of N and P doping and unique architecture of the N, P-CNT array. This construction of robust CNTs nanostructure for the designed electrocatalytic application and other potential application will find a broad interest in scientific and industrial fields.

Acknowledgments

This work was supported by the Major International (Regional) Joint Research Project (51210002), the Link Project of the National Natural Science Foundation of China and Guangdong Province (U1034003), the National Natural Science Foundation of China (21073241, 21201058) and the Australian Research Council (DP120102325 and DP120104932).

Notes and references

[a] *State Key Laboratory of Optoelectronic Materials and Technologies, and Key Laboratory of Low-carbon Chemistry & Energy Conservation of Guangdong Province, School of Physics and Engineering, Sun Yat-sen University, 135 Xingang Road, Guangzhou, 510275, PR China. Fax: (+8620)-84036736; Tel: (+8620)-84036736; E-mail: stsspk@mail.sysu.edu.cn*

[b] *Fuels and Energy Technology Institute & Department of Chemical Engineering, Curtin University, Perth, WA6102, Australia. E-mail: s.jiang@curtin.edu.au*

[c] *Key Laboratory of Functional Inorganic Material Chemistry, Ministry of Education of the People's Republic of China, Heilongjiang University, Harbin, 150080, P. R. China.*

† Electronic Supplementary Information (ESI) available: [details of any supplementary information available should be included here]. See DOI: 10.1039/b000000x/

1 D. M. Guldi. *Chem Commun* 2000, 321.
2 D. Tasis, N. Tagmatarchis, A. Bianco, M. Prato. *Chem. Rev.* 2006, **106**, 1105.
3 K. Gong, F. Du, Z. Xia, M. Durstock, L. Dai. *Science* 2009, **323**, 760.
4 M. Matsui, N. Takahashi, J.-i. Ozaki. *Carbon* 2011, **49**, 4505.
5 S. J. Teng, J. N. Wang, X. X. Wang. *J Mater Chem* 2011, **21**, 5443.
6 U. N. Maiti, S. Maiti, N. S. Das, K. K. Chattopadhyay. *Nanoscale* 2011, **3**, 4135.
7 B. Assfour, S. Leoni, G. Seifert, I. A. Baburin. *Adv Mater* 2011, **23**, 1237.
8 B. J. Landi, M. J. Ganter, C. D. Cress, R. A. DiLeo, R. P. Raffaelle. *Energ Environ Sci* 2009, **2**, 638.
9 N. Jha, P. Ramesh, E. Bekyarova, M. E. Itkis, R. C. Haddon. *Adv Energy Mater* 2012, **2**, 438.
10 H. Orikasa, N. Inokuma, S. Ittisanronnachai, X.-H. Wang, O. Kitakami, T. Kyotani. *Chem Commun* 2008, 2215.
11 R. Kitaura, N. Imazu, K. Kobayashi, H. Shinohara. *Nano Lett* 2008, **8**, 693.
12 C. Xiong, Z. Wei, B. Hu, S. Chen, L. Li, L. Guo, et al. *J Power Sources* 2012, **215**, 216.
13 Z. Jin, H. Nie, Z. Yang, J. Zhang, Z. Liu, X. Xu, et al. *Nanoscale* 2012, **4**, 6455.
14 L. Yang, S. Jiang, Y. Zhao, L. Zhu, S. Chen, X. Wang, et al. *Angewandte Chemie* 2011, **123**, 7270.
15 D. Yu, Y. Xue, L. Dai. *J. Phys. Chem. Lett*. 2012, **3**, 2863.
16 D. Geng, Y. Chen, Y. Chen, Y. Li, R. Li, X. Sun, et al. *Energy. Environ. Sci*. 2011, **4**, 760.
17 X. Sun, Y. Zhang, P. Song, J. Pan, L. Zhuang, W. Xu, et al. *Acs Catal* 2013, **3**, 1726.
18 Z. Yang, Z. Yao, G. Li, G. Fang, H. Nie, Z. Liu, et al. *Acs Nano* 2011, **6**, 205.
19 B. Shan, K. *Cho. Chem. Phys. Lett*. 2010, **492**, 131.
20 Y. Tan, C. Xu, G. Chen, X. Fang, N. Zheng, Q. Xie. *Adv Funct Mater* 2012, **22**, 4584.
21 Y. Zheng, Y. Jiao, M. Jaroniec, Y. Jin, S. Z. Qiao. *Small* 2012, **8**, 3550.
22 Y. Zhao, L. Yang, S. Chen, X. Wang, Y. Ma, Q. Wu, et al. *J Am Chem Soc* 2013, **135**, 1201.
23 Z. Wang, R. Jia, J. Zheng, J. Zhao, L. Li, J. Song, et al. *Acs Nano* 2011, **5**, 1677.
24 S. Lim, H. Elim, X. Gao, A. Wee, W. Ji, J. Lee, et al. *Phys Rev B* 2006, **73**, 045402.
25 T. Sharifi, G. Hu, X. Jia, T. Wågberg. *Acs Nano* 2012, **6**, 8904.
26 L. Feng, Y. Yan, Y. Chen, L. Wang. *Energ Environ Sci* 2011, **4**, 1892.
27 E. Cruz-Silva, D. A. Cullen, L. Gu, J. M. Romo-Herrera, E. Muñoz-Sandoval, F. López-Urías, et al. *Acs Nano* 2008, **2**, 441.
28 Y. Zhang, J. Ge, L. Wang, D. Wang, F. Ding, X. Tao, et al. *Sci Rep* 2013, **3**, 2771.
29 L. Song, S. Zhang, Q. Wei. *J Solid State Chem* 2011, **184**, 1556.
30 R. Scholder, A. Apel, H. Haken. *Z Anorg Allg Chem* 1937, **232**, 1.
31 Z. Zhu, Y. Lu, D. Qiao, S. Bai, T. Hu, L. Li, et al. *J Am Chem Soc* 2005, **127**, 15698.
32 J. P. Tessonnier, D. S. Su. *Chemsuschem* 2011, **4**, 824.
33 X. Wu, Y. Tao, Y. Lu, L. Dong, Z. Hu. *Diam Relat Mater* 2006, **15**, 164.
34 M. Lin, J. P. Y. Tan, C. Boothroyd, K. P. Loh, E. S. Tok, Y.-L. Foo. *Nano Lett* 2007, **7**, 2234.
35 S. Trasobares, O. Stephan, C. Colliex, W. Hsu, H. Kroto, D. Walton. *J. Chem. Phys*. 2002, 116, 8966.
36 M. B. Jakubinek, M. A. White, G. Li, C. Jayasinghe, W. Cho, M. J. Schulz, et al. *Carbon* 2010, **48**, 3947.
37 M. He, S. Vasala, H. Jiang, M. Karppinen, E. I. Kauppinen, M. Niemelä, et al. *Carbon* 2012, **50**, 4750.
38 K. Ghosh, M. Kumar, T. Maruyama, Y. Ando. *Carbon* 2009, **47**, 1565.
39 J. Zhu, Y. Li, S. Kang, X. We, P. K. Shen, *J Mater Chem A* 2014, **2**, 3142.
40 H.-P. Cong, P. Wang, M. Gong, S.-H. Yu. *Nano Energy* 2014, **3**, 55.
41 C. H. Choi, M. W. Chung, S. H. Park, S. I. Woo. *Rsc Adv* 2013, **3**, 4246.
42 Y. Shao, S. Zhang, M. H. Engelhard, G. Li, G. Shao, Y. Wang, et al. *J Mater Chem* 2010, **20**, 7491.
43 J. Zhu, C. He, Y. Li, S. Kang, P. K. Shen. *J Mater Chem A* 2013, **1**, 14700.
44 O. S. Panwar, M. A. Khan, M. Kumar, S. M. Shivaprasad, B. S. Satyanarayana, P. N. Dixit, et al. *Jpn J Appl Phys* 2009, **48**, 5501.
45 D.-S. Yang, D. Bhattacharjya, S. Inamdar, J. Park, J.-S. Yu. *J Am Chem Soc* 2012, **134**, 16127.
46 S. Wang, E. Iyyamperumal, A. Roy, Y. Xue, D. Yu, L. Dai. *Angewandte Chemie International Edition* 2011, **50**, 11756.
47 J. Zhu, P. K. Shen. *Rsc Adv* 2013, **3**, 14686.
48 Z. W. Liu, F. Peng, H. J. Wang, H. Yu, W. X. Zheng, J. Yang. *Angewandte Chemie* 2011, **123**, 3315.

This journal is © The Royal Society of Chemistry [year]

49 G. He, Z. Yan, X. Ma, H. Meng, P. K. Shen, C. Wang. Nanoscale 2011, **3**, 3578.

GA image

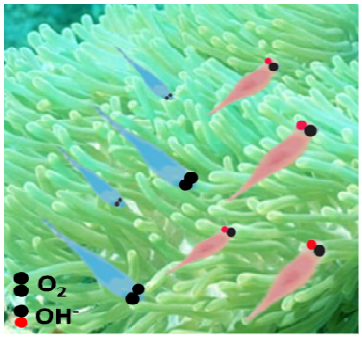

The N, P-dual-doped CNTs with a robust nano-structure has been synthesized by one-pot method and the material shows enhanced activities and durability for oxygen reduction reaction.